

N89-21747

1988

NASA/ASEE SUMMER FACULTY FELLOWSHIP PROGRAM

MARSHALL SPACE FLIGHT CENTER  
THE UNIVERSITY OF ALABAMAFLUCTUATION ANALYSIS OF RELATIVISTIC NUCLEUS-NUCLEUS  
COLLISIONS IN EMULSION CHAMBERS

Prepared by:	Stephen C. McGuire
Academic Rank:	Associate Professor
University and Department:	Alabama A&M University Department of Physics
NASA/ASEE:	
Laboratory:	Space Science
Division:	Astrophysics
Branch:	High Energy Astrophysics
NASA Colleague:	Thomas A. Parnell
Date:	August 15, 1988
Contract No.:	NGT 01-002-099 The University of Alabama

FLUCTUATION ANALYSIS OF RELATIVISTIC NUCLEUS-NUCLEUS  
COLLISIONS IN EMULSION CHAMBERS

by

Stephen C. McGuire  
Associate Professor of Physics  
Alabama A&M University  
Normal, Alabama 35762

ABSTRACT

We have developed an analytical technique for identifying enhanced fluctuations in the angular distributions of secondary particles produced from relativistic nucleus-nucleus collisions. The method is applied under the assumption that the masses of the produced particles are small compared to their linear momenta. The importance of this work rests in the fact that enhanced fluctuations in the rapidity distributions is considered to be an experimental signal for the creation of the quark-gluon-plasma(QGP), a new state of nuclear matter predicted from quantum chromodynamical theory(QCD). In our approach, Monte Carlo simulations are employed that make use of a portable random number generator that allow the calculations to be performed on a desktop computer. The method is illustrated with data taken from high altitude emulsion exposures and is immediately applicable to similar data from accelerator-based emulsion exposures.

### ACKNOWLEDGEMENTS

I am very grateful to Thomas A. Parnell and James H. Derrickson for serving as my colleagues and for providing valuable technical guidance during my appointment as a NASA/ASEE Summer Faculty Fellow. Many thanks go to Yoshi Takahashi for making data from the EMU05 experiment available to me for analysis. The administrative assistance and financial support of the NASA/ASEE Summer Faculty Fellowship Program, Michael L. Freeman, director and Ernestine Cothran, co-director, is gratefully acknowledged.

## LIST OF FIGURES

- Figure 1. Cross sectional view of the emulsion chamber configuration designated as 5A2 for the EMU05 experiment showing its internal components.
- Figure 2. Coordinate system sketch showing the relationship between the linear momentum,  $p$ , of a secondary particle and its projection  $p_{||}$ , along the direction of the primary nucleus.
- Figure 3. Experimental pseudorapidity distribution for event 6-869. The solid curve is the result of a least squares fit of the data to the function:

$$f_s^4(\eta) = a_0/2 + \sum_{i=1}^4 a_k T_k(\eta).$$

where the  $T_k$  are Chebyshev polynomials of the first kind.

- Figure 4. Distribution of the V-fluctuations for a 1000 event simulation of 6-869. The smooth solid curve is a fit to a gaussian,  $y(x) = a_1 \exp[(-1/2)\{(x - a_2)/a_3\}^2]$ , where  $a_1 = 100.2 \pm 0.49$ ,  $a_2 = 318.7 \pm 0.28$  and  $a_3 = 55.4 \pm 0.29$ . The uncertainties in the parameters are purely statistical and correspond to one standard deviation.
- Figure 5. Distribution of the S-fluctuations for a 1000 event simulation of 6-869. The smooth solid curve is a fit to a gaussian,  $y(x) = a_1 \exp[(-1/2)\{(x - a_2)/a_3\}^2]$ , where  $a_1 = 144.1 \pm 0.56$ ,  $a_2 = 2800.0 \pm 0.38$  and  $a_3 = 839.0 \pm 3.83$ . The uncertainties in the parameters are purely statistical and correspond to one standard deviation.

## INTRODUCTION

In recent years much interest has developed in the detailed study of collisions between nuclei at relativistic energies because it provides a microscopic laboratory for examining the basic structure of nuclear matter. This basic structure is perhaps best described in terms of the quark-model of matter. Quarks themselves are believed to be the most fundamental constituents of matter from which more complex particles are constructed. At normal nuclear densities they are bound together strongly in a given combination by other particles referred to as gluons. If, however, the energy density inside the nucleus can be raised to about 2-3 times its normal value, the theory of quantum chromodynamics<sub>1</sub> (QCD) predicts that nuclear matter will undergo a marked phase change<sup>1</sup>. In the new phase, quarks and gluons are freed from each other to form a kind of ideal gas or plasma of particles currently referred to as the quark-gluon plasma (QGP). At even higher energy densities the plasma is expected to more closely approximate an ideal gas. The detailed properties of the QGP and the precise mechanisms(s) by which it is produced are not well understood at the present time and therefore merit thorough investigation.

As with most experimental efforts aimed at probing the structure of nuclear matter, we seek to determine the nature of the medium by careful examination of the properties of the particles produced by the collision. These physical quantities include the average transverse momentum, multiplicities, angular distribution structure and energy densities. Nucleus-nucleus collisions have an advantage over experiments involving lighter particles in that higher energy densities and larger particle multiplicities are produced on the average. Larger multiplicities mean that statistical fluctuations in the angular distributions should be smaller and correlated behavior should be more obvious<sup>2</sup>. Indeed, one of the expected experimental signals for the creation of the QGP in a relativistic collision is the occurrence of enhanced fluctuations in the<sub>3,4</sub> rapidity distributions of the secondary particles that are generated<sup>3,4</sup>. Further, structures in the angular distributions of produced particles have been<sub>5,6</sub> shown to contain evidences of collective flow of nuclear matter<sup>5,6</sup>.

In this report we present a theoretical method for identifying nonstatistical fluctuations in the pseudorapidity distributions of individual events. An example of its application to data obtained from a high-altitude emulsion detector experiment is given. Further, accelerator-based experiments, involving the exposure of emulsion chambers to relativistic beams of oxygen and sulphur, are described. The latter hold the promise of providing data to help illuminate the physics of the system of colliding nuclei.

## OBJECTIVES

The principal objective of this project is to analyze and interpret secondary particle distribution data, recorded in emulsion detectors, for the existence of nonstatistical structure. Attention is focussed on collisions between nuclei at relativistic and ultrarelativistic energies. Methods are to be developed that facilitate the reduction of data, test prevailing models of the collision process and suggest new ways of viewing data from accelerator-based experiments.

## EXPERIMENT DESCRIPTION

Emulsion detectors that are used in this project are designed fundamentally to help determine the charge and paths of the particles that traverse them. The charges of the particles are identified partly from the ionization damage they produce in the CR39 plastic plates. The detector is operated inside of a uniform, constant magnetic field so that the curvature of the path indicates the sign of the charge and provides data on the momentum of the particle transverse to the beam direction.

A sketch of the experimental arrangement, showing the approximate dimensions of the chamber and its component parts is provided in figure 1. Each emulsion plate has a 70  $\mu\text{m}$  base coated on both sides with 50  $\mu\text{m}$  of emulsion. The separation between the plates is not a constant but gradually increases in the direction of the beam. This feature facilitates the measurement of the track curvature and the direction of deflection for the emitted particle. Lead plates are placed near the front of the detector where the density of emulsions plates is greater to increase the likelihood of interactions there. The larger density of emulsion plates also improves the accuracy with which the position of the collision vertex and emission angles can be determined. Low density, styrofoam spacers are used in the rear sections of the detector to maintain the separation between the emulsion plates.

Pulsed beams of  $^{32}\text{S}$  ions at 200 GeV/nucleon were provided by the Super Proton  $\gamma$ -Synchrotron (SPS) accelerator of the European Center for Nuclear Research. The duration of each pulse was 2s with a total intensity of  $3 \times 10^3$  ions/cm<sup>2</sup>/pulse. The beam size was 2.54cm x 2.54cm and the chamber was exposed to beam spills shifted laterally from each other by 1 cm.

## THEORY

### Relationship Between the Rapidity and the Pseudorapidity:

We have chosen to express the distributions in terms of the pseudorapidity variable, a convenient form for which is derived below.

The value of the rapidity associated with a secondary particle is given by the equation

$$y = (1/2)\ln[(E + p_{||})/(E - p_{||})] \quad . \quad (1)$$

E is the total energy of the particle and  $p_{||}$  is the component of its linear momentum parallel to the direction of the incident nucleus. Using the cartesian coordinate system shown in figure 2, y can be expressed as

$$y = (1/2)\ln\left\{\frac{\sqrt{p^2 + m^2} + p\cos\theta}{\sqrt{p^2 + m^2} - p\cos\theta}\right\} \quad , \quad (2)$$

where  $E = \sqrt{p^2 + m^2}$  and  $p_{||} = p\cos\theta$ . In the limit of  $m/p \ll 1$ , equation (2) can be approximated by

$$y \approx (1/2)\ln[(1 + \cos\theta)/(1 - \cos\theta)] \quad , \quad (3)$$

where we now can make the definition of a new variable,

$$\eta = -\ln[(1 - \cos\theta)/(1 + \cos\theta)]^{1/2} \quad , \quad (4)$$

the pseudorapidity. Using the trigonometric half-angle identity,

$$\tan(\theta/2) = [(1 - \cos\theta)/(1 + \cos\theta)]^{1/2} \quad , \quad (5)$$

equation 4 simply becomes

$$\eta = -\ln[\tan(\theta/2)] \quad . \quad (6)$$

Since  $\eta$  does represent an approximation to y, care must be taken in choosing an appropriate bin size in constructing the distribution in  $\eta$  such that the character of the fluctuations will be preserved. Too large a bin width can have the effect of masking important structure, and too small a bin size can produce artificial variations in particle intensity. For practical purposes, the bin width,  $\Delta\eta$ , is chosen to match the resolution with which the values of the polar scattering angle can be determined. Use of  $\eta$  has the clear advantage that it is not necessary to know the mass of the secondary particle. It does,

however, rely on the accurate measurement of the laboratory scattering angles,  $\theta_i$ , for the produced particles.

The values of  $\theta_i$  are found from the cartesian coordinates of the tracks recorded by the emulsions. We have written a set of algorithms that perform this conversion using a conceptually simple procedure. Since the path of the particles are curved, an nth order polynomial is used to find the least squares fit to a each  $[x_i, y_i]$  data set corresponding to a particular track. At present, the maximum value of n is 10. The polar emission angle,  $\theta_i$ , is then estimated by calculating the tangent to the curve near the interaction vertex. The algorithms have been programmed in BASIC on a desktop computer and are written to be machine independent for portability.

Definition of the Fluctuation:

Two definitions of the fluctuation, given below, are used for this part of the analysis. In what follows L is the number of bins in the experimental distribution and  $f(\eta_i)$  is the intensity in the ith bin.

$$I. \quad V_{\text{exp}} = \sum_{i=1}^{L+1} |f(\eta_i) - f(\eta)_{i-1}| \quad , (7)$$

where  $f(\eta_0) = f(\eta_{L+1}) = 0$ .

$$II. \quad S_{\text{exp}} = \sum_{i=1}^L [f(\eta)_i - f_s(\eta)_i]^2 \quad . (8)$$

Both of these expressions possess a minimum value of zero corresponding to the case where no fluctuations are present. Form I. is the total vertical length of the distribution and form II. gives a measure of the total deviation from a function  $f_s$  which describes the average features of the distribution. The function  $f_s$  is found by fitting the data to a superposition of Chebyshev polynomials.

Using the form of the function,  $f_s$ , obtained from the fit, the experimental distribution for a given event is simulated a large number of times with a Monte Carlo procedure. For each simulation the number of secondary particles is held fixed to the observed value, and the fluctuations, given by equations 7 and 8 above, are computed and saved. Thus, a collection of values of V and S are generated for each set of simulations. When many simulations are used, the distributions



in  $V$  and  $S$  are expected to have a gaussian shape, in accordance with the central limit theorem.

### APPLICATION OF METHODS AND RESULTS

In this section we give an example of the application of the theory, with results from a relativistic nucleus-nucleus collision. The data are from an event observed in emulsions that were flown at high atmospheric altitude in an experiment designed to study the heavy-ion component of the cosmic ray spectrum. The design<sup>10</sup> and operation of the detector have been described in detail elsewhere<sup>11</sup>. The event involved the interaction of an iron nucleus with the emulsion at 54 GeV/nucleon that produced 132 secondary particles. Initial interest in this event stemmed in part from an unusual bimodal structure in its particle intensity in the azimuthal direction<sup>11</sup>. Prompted by the predictions of QCD, the possibility of related structure was anticipated in the polar direction. In figure 3, a histogram of the experimental pseudorapidity distribution for the event is plotted together with the function,  $f^4$ , obtained by fitting the data to a polynomial given by

$$f^4 = v_0/2 + \sum_{k=1}^4 a_k T_k, \quad (9)$$

where  $T_k$  are Chebyshev polynomials of the first kind. The bin width was chosen to be 0.2 units of  $\eta$ . By randomly sampling  $f^4$ , the experimental distribution was simulated 1000 times. A desktop personal computer, programmed in FORTRAN was used for this part of the calculation. The computer was equipped with a math coprocessor that reduced the time otherwise required for the calculations by a factor of 8 to 10. Central to the accuracy of the simulations is the reliability of the pseudorandom number generator. Its performance was evaluated by comparing the fluctuation distributions in  $V$  and  $S$  to an expected gaussian shape. The solid curve drawn on the histograms in figures 4 and 5 represents the result of a least squares fit of the data to a gaussian. The two plots are seen to be in good agreement with each other. Also shown on each figure is the location of the experimental value of the fluctuation. In each case it falls within the half-width of the theoretical curve, thus providing a strong indication that the intensity variations in the experimental distribution are likely due to statistical sources. The location of the experimental fluctuations within the probability distributions is by no means an expected result. It is, however, one which must be supported by predictions of reaction products based on deterministic models of the collision process. To this end, it is important that the analysis be extended to experiments that involve many central collisions of the same type that have higher numbers of produced particles and whose energy densities exceed the threshold values for QGP production.

## CONCLUSIONS AND RECOMMENDATIONS

The methods described in this report places on a firm quantitative basis the identification of enhanced fluctuations in secondary particle distributions. The technique is general, in that it can be applied to any one-dimensional distribution. At present, the physical mechanisms for QGP production are not well understood. Therefore there continues to be a need for additional theoretical work that couple statistical analyses with deterministic modelling of the collision process. These investigations will rely mainly upon nucleus-nucleus collision data obtained at ground-based heavy-ion accelerators. It is expected, however, that information from accelerator experiments will complement data obtained from high-altitude emulsion detector exposures<sup>13</sup>.

One example of an event currently under examination is the collision, <sup>32</sup>S+Pb, at 200 GeV/nucleon. The collision was observed in the 5A2 emulsion detector during an exposure at CERN. Because of its energy and multiplicity ( $N_s=399$ ), it is an excellent case for our analysis. Unfortunately, the process by which the emulsion plates are scanned to obtain the track coordinate data is not computerized, making the calculation of the individual secondary particle emission angles a time-consuming step of the process. An automated system for scanning the emulsion plates, computerizing the coordinate data and converting it to emission angles is therefore a strongly recommended addition to this project.

## REFERENCES

1. E. Shuryak, Quantum Chromodynamics and the Theory of Superdense Matter. Phys. Rep. 61C:71,1980.
2. L. McLerran and B. Svetitsky, American Scientist, Vol. 75, p. 490, 1987.
3. Physics Today, Vol. 4, No. 1, January, 1988, S-56.
4. M. D. Slaughter, LA-UR 88-617.
5. J. A. Zingman et al., Phys. Rev. C, Vol. 38, No. 2,(1988). p. 760.
6. P. L. Jain, K. Sengupta and G. Singh, Phys. Rev. C, Vol. 37, No. 2, 1988, p. 63.
7. Y. Takahashi et al.,CERN Experiment Proposal, CERN/SPSC 85-50, SPSC/P216S.
8. M. Abramowitz and I. Stegun, Handbook of Mathematical Functions, NBS/APS No. 55, Nov. 1970, p. 795.
9. W. T. Eadie et al., Statistical Methods in Experimental Physics, North Holland, Amsterdam, 1971, p. 124.
10. T. H. Burnett et al., Phys. Rev. D, Vol 35, No. 3,(1987), p. 824.
11. W. V. Jones et al., Ann. Rev. Nucl. Sci., 1987, 37:71-95.
12. S. C. McGuire, NASA Contractor Report No. 4054, March,1987,pp. 10-16.
13. Y. Takahashi, Nucl. Phys., A478,(1988), 675c-683c.

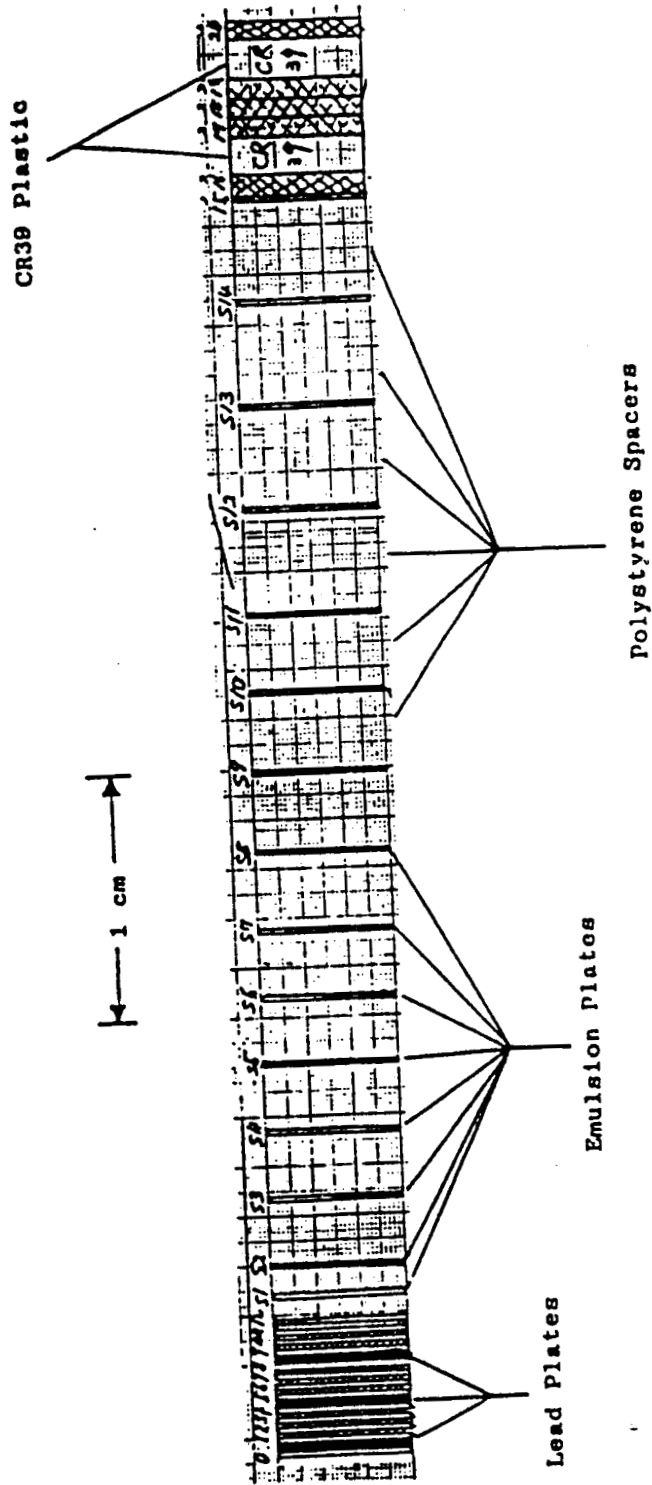


Figure 1.

ORIGINAL PAGE IS  
OF POOR QUALITY

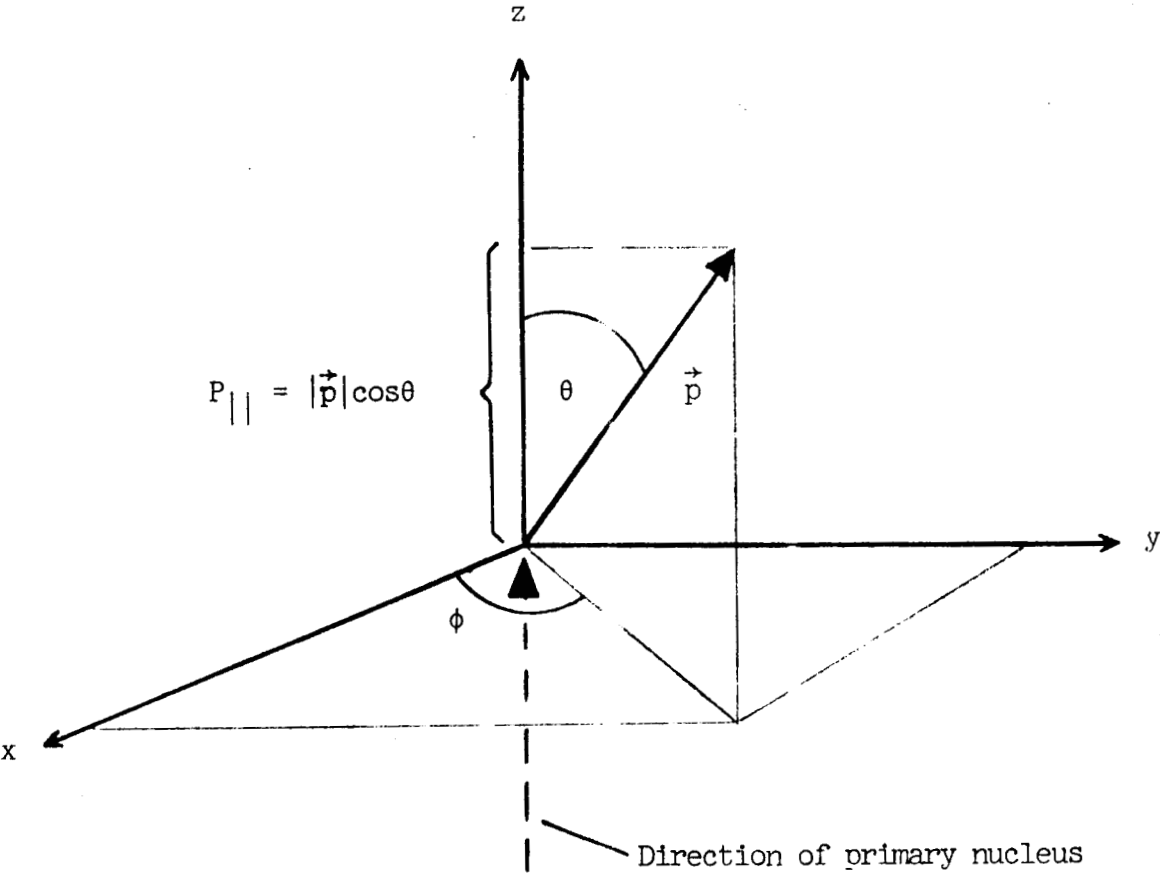


Figure 2.

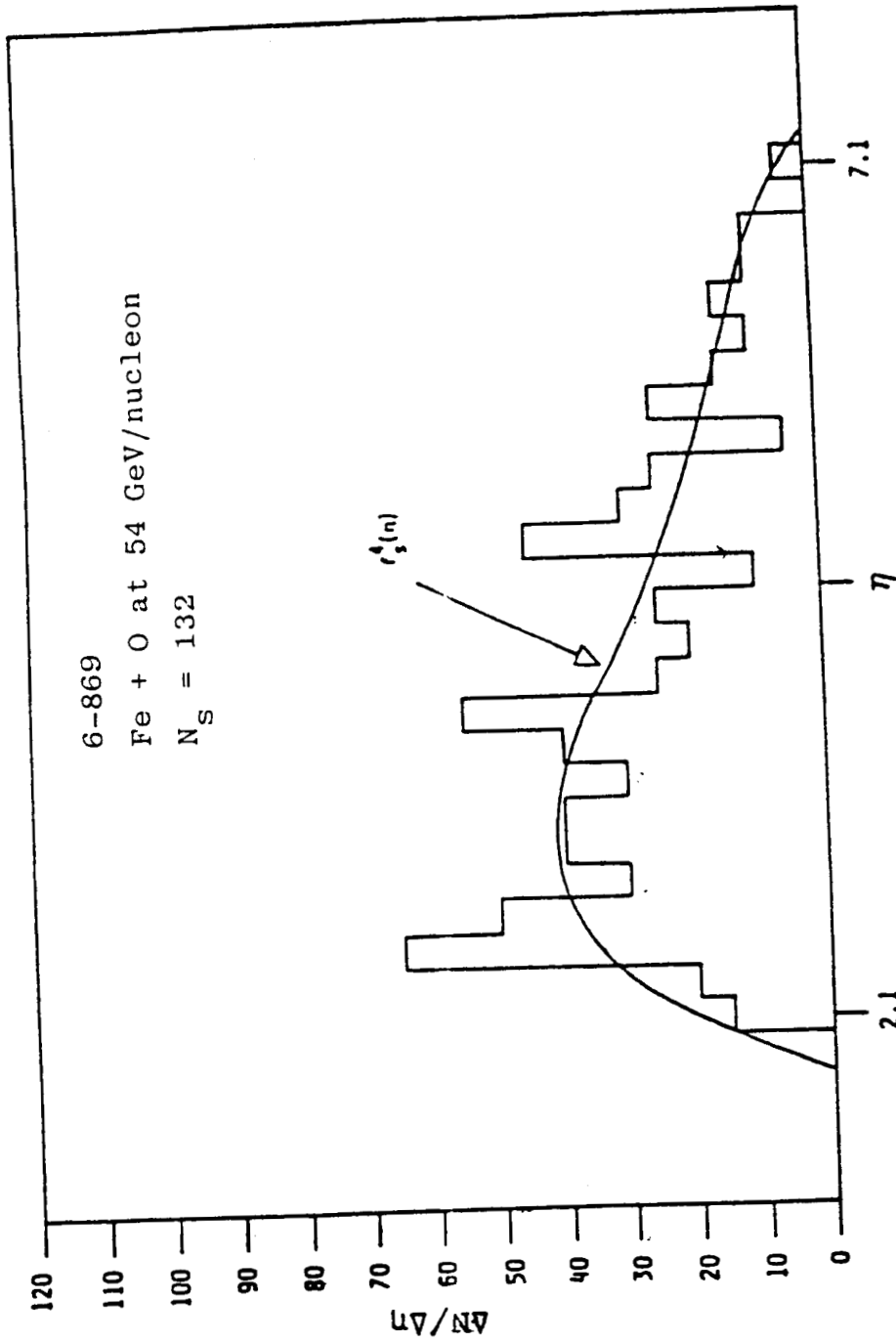


Figure 3.

ORIGINAL PAGE IS  
 OF POOR QUALITY

ORIGINAL PAGE IS  
OF POOR QUALITY

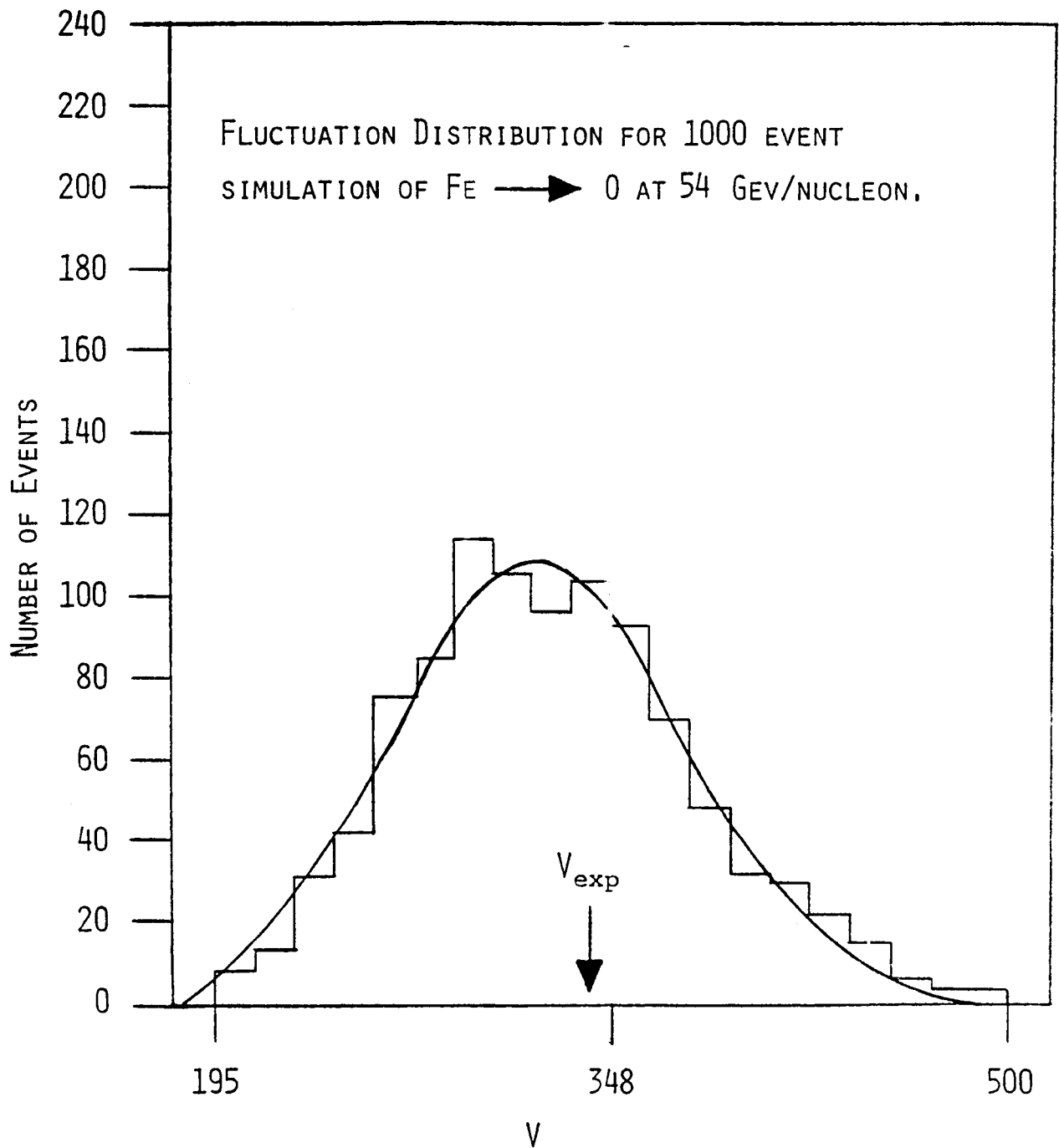


Figure 4.

XXI-11

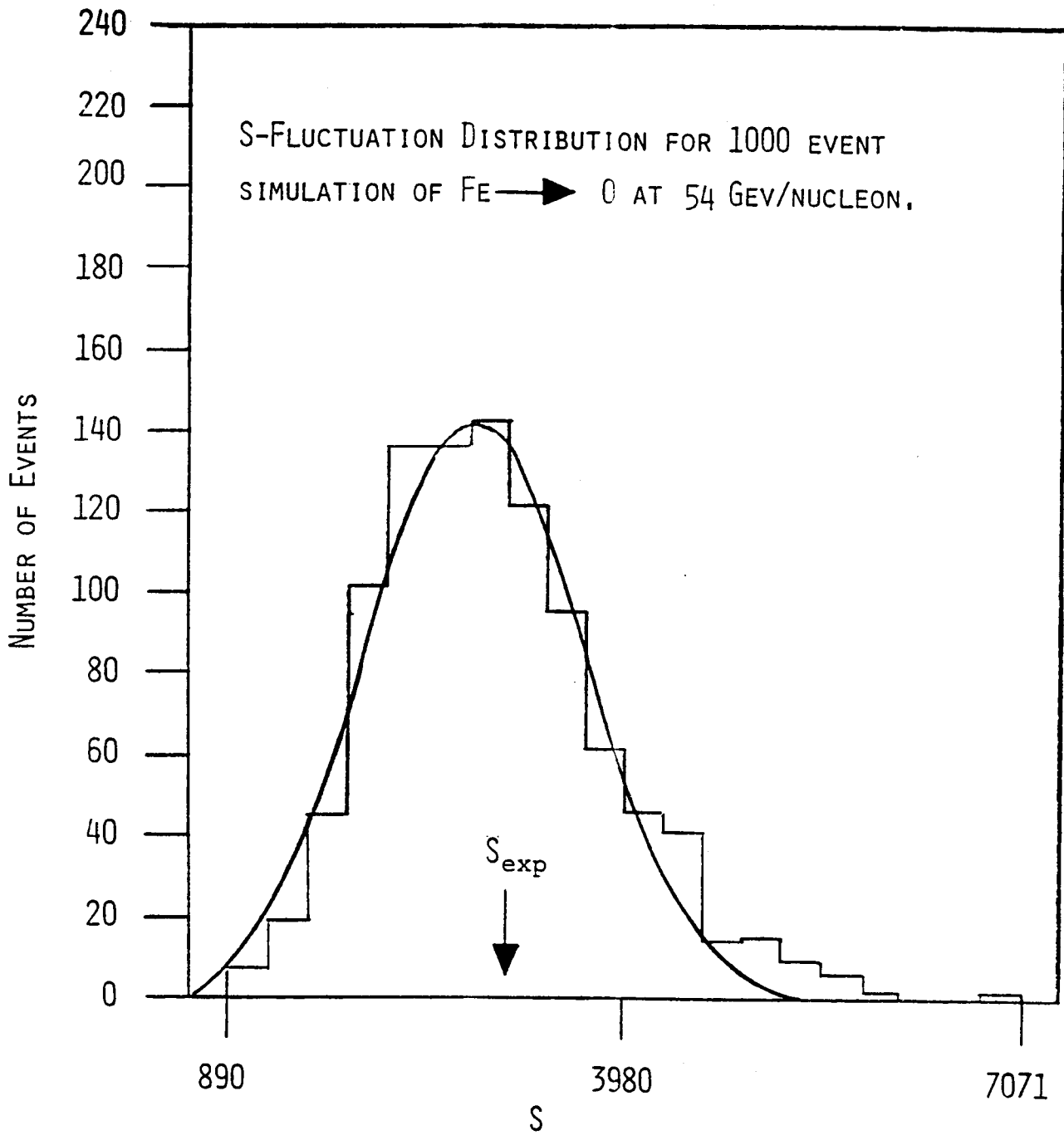


Figure 5.  
XXI-12